ELSEVIER

Computer Aided Geometric Design 19 (2002) 645–662

COMPUTER AIDED GEOMETRIC DESIGN

www.elsevier.com/locate/cagd

Triangular patch modeling using combination method

Caiming Zhang [*,1], Fuhua (Frank) Cheng [2]

Department of Computer Science, University of Kentucky, Lexington, KY 40506-0046, USA

Received 20 September 2000; received in revised form 28 January 2002

Abstract

A new method for constructing triangular patches is presented. A triangular patch that interpolates given boundary curves and cross-boundary slopes is formed by blending three traditional side-vertex interpolation operators (Nielson, 1979) with a new, *interior interpolation operator*. The new operator is the solution of an interpolation process that interpolates both the interior and the boundary of the triangular domain. The interior interpolation operator has better approximation precision on the interior of the triangle than the side-vertex operators. The constructed triangular patch reproduces polynomial surfaces of degree four. Comparison results of the new method with the side-vertex method (Nielson, 1979) are included.

Keywords: Triangular patch; Interpolation; Quartic polynomial; Combination method; Interior interpolation operator; Side-vertex interpolation operator

1. Introduction

In the fields of CAD and free-form surface modeling, the construction of surfaces plays an important role. To make the process of constructing complex surfaces simple, piecewise techniques are frequently used, with four-sided and triangular patches being the most popular choices. This paper discusses the process of constructing a curved triangular patch that interpolates given boundary curves and cross-boundary slopes.

The first smooth interpolant to boundary curves of a triangle was proposed by Barnhill, Birkhoff and Gordon (1973). The triangular patch is constructed using the *Boolean sum scheme*. After their method,

[*] Corresponding author.
E-mail address: czhang@csr.uky.edu (C. Zhang).

[1] Supported by Ford and Honda. Currently with the School of Computer Science and Technology, Shandong University, China.

[2] Supported by NSF(9722728), Ford and Honda.

0167-8396/02/$ – see front matter
PII: S0167-8396(02)00148-6

several other papers have discussed the boundary curve interpolation problem for triangular patches. Gregory (1974) introduced the *convex combination method* into computer aided geometric design and the idea was further developed in papers (Charrot and Gregory, 1984; Gregory, 1983). To construct a triangular patch, three interpolation operators each of which satisfies the interpolation conditions on two sides of a triangle are constructed, the combination of the three interpolation operators forms the curved triangular patch.

Nielson (1979) presented a *side-vertex method for* constructing a curved triangular patch using combination of three interpolation operators, each satisfying the given interpolation conditions at a vertex and its opposite side. Based on operators similar to Nielson's approach, Hagen (1986) developed a method for constructing *geometric surface patches.* These results have been generalized to triangular surface patches with first and second order geometric continuity (Hagen, 1989; Nielson, 1987). The method in (Foley and Opitz, 1992) is developed for *scattered data interpolation.* Its conversion process works for constructing curved triangular patches. The problem of constructing curved triangular patches is also studied in (Kuriyama, 1994; Varady, 1991; Zhang et al., 1993).

The common point of the methods (Charrot and Gregory, 1984; Gregory, 1974, 1983; Hagen, 1986; Nielson, 1979) is that three interpolation operators are used to construct a curved triangular patch and these interpolation operators consider interpolation conditions on the boundary of the triangular domain only. This paper presents a method to construct a curved triangular patch by combining four interpolation operators: an *interior interpolation operator* and three *side-vertex operators* (Nielson, 1979). The construction of the new interpolation operator is different from traditional interpolation operators in that interpolation conditions are not only set for the boundary but also the interior of the triangular domain. This is achieved by requiring three quartic curves (actually, surfaces) to be tangent to a plane at their intersection point. This is a new approach in surface construction. While the side-vertex operators have better approximation precision for areas close to the boundary edges of the triangle, the interior interpolation operator has better approximation precision for the interior of the triangle. The constructed triangular patch satisfies C^1 boundary condition and reproduces polynomial surfaces of degree four. The new method can also be extended to construct C^2 triangular patches by replacing Nielson's side-vertex operators with Hagen's interpolation operators (Hagen, 1986).

The rest of the paper is arranged as follows. In Section 2, the problem to be studied is formulated and the basic idea of the new method is described. In Section 3, the construction process of the interior interpolation operator using three quartic curves is described. The construction of a triangular patch by combining four interpolation operators is discussed in Section 4. Comparison results of the new method with Nielson's approach (1979) are shown in Section 5. The concluding remarks are given in Section 6.

2. Problem formulation and basic idea

Let T be a triangle with vertices $\boldsymbol{v}_i = (x_i, y_i)$, $i = 1, 2, 3$, in the xy-plane, and e_i denote the opposite side of $\boldsymbol{v}_i$, as shown in Fig. 1. The goal here is to construct a function $P_T(x, y)$ on the triangular domain T that interpolates given C^1 boundary curves and cross-boundary slopes. Without loss of generality, we shall assume that the given boundary curves and cross-boundary slopes are taken from a C^1 function $F(x, y)$ defined on T. The constructed triangular function would reproduce polynomial surfaces of degree four, that is, if $F(x, y)$ is a polynomial surface of degree four on T and if $P_T(x, y)$ agrees with $F(x, y)$ and its cross-boundary slopes on the bounding edges of T, then $P_T(x, y) = F(x, y)$ on T.

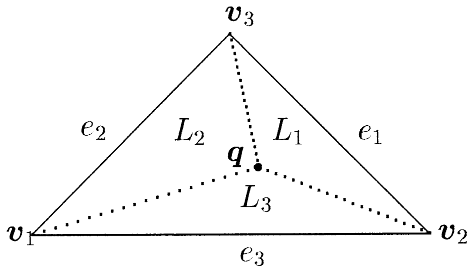

Fig. 1. Area coordinates with respect to T.

The construction process of $P_T(x, y)$ consists of two steps. First, an *interior interpolation operator* $P(x, y)$ defined on T is constructed. The construction of this interpolation operator is to ensure that the interior shape of the resulting triangular patch is also a consideration factor in the construction process of the triangular patch. $P(x, y)$ interpolates the given boundary curves but may not interpolate the given cross-boundary slopes. The desired triangular patch $P_T(x, y)$ is then formed by combining $P(x, y)$ with three *side-vertex operators* defined by Nielson (1979). In addition to ensuring that the required interpolation conditions are satisfied by the constructed triangular patch, the combination process is also arranged in a way so that the shape of $P_T(x, y)$ is primarily determined by $P(x, y)$, while the side-vertex operators $N_i(x, y)$, $i = 1, 2, 3$, are mainly used as transition surface patches to make the connection of $P_T(x, y)$ with adjacent surface patches smooth.

Barycentric coordinates will be used in this work to construct the triangular patch $P_T(x, y)$. Given a point $\boldsymbol{q}$ of T, the barycentric coordinates of $\boldsymbol{q}$ with respect to T (see Fig. 1), denoted (L_1, L_2, L_3), satisfy the following properties: (1) L_i is a linear function with value one at $\boldsymbol{v}_i$ and zero along the side e_i; (2) $\boldsymbol{q} = L_1\boldsymbol{v}_1 + L_2\boldsymbol{v}_2 + L_3\boldsymbol{v}_3$.

3. Interior interpolation operator

The construction of the interior interpolation operator is based on that of three quartic curves. The construction of these quartic curves is described first.

3.1. Constructing quartic curves

Given an arbitrary point $\boldsymbol{q} = (x, y)$ of T, let $\boldsymbol{q} = (\bar{x}_i, \bar{y}_i)$ be the intersection point of the side e_i with the line that passes through $\boldsymbol{v}_i$ and $\boldsymbol{q}$, $i = 1, 2, 3$, as shown in Fig. 2. If (L_1, L_2, L_3) are the barycentric coordinates of $\boldsymbol{q}$ with respect to T, then we have $\boldsymbol{q}_1 = \frac{L_2\boldsymbol{v}_2 + L_3\boldsymbol{v}_3}{L_2 + L_3}$, $\boldsymbol{q}_2 = \frac{L_1\boldsymbol{v}_1 + L_3\boldsymbol{v}_3}{L_1 + L_3}$ and $\boldsymbol{q}_3 = \frac{L_1\boldsymbol{v}_1 + L_2\boldsymbol{v}_2}{L_1 + L_2}$, respectively.

The direction vector from $\boldsymbol{v}_i$ to $\boldsymbol{q}_i$ is denoted by n_i. The given function values and derivatives along the direction n_i at $\boldsymbol{v}_i$ and $\boldsymbol{q}_i$ are denoted by $F(\boldsymbol{v}_i)$, $\frac{\partial F(\boldsymbol{v}_i)}{\partial n_i}$, $F(\boldsymbol{q}_i)$ and $\frac{\partial F(\boldsymbol{q}_i)}{\partial n_i}$, respectively, $i = 1, 2, 3$.

Let $P(\boldsymbol{q}) = P(x, y)$ denote the value of the interior interpolation operator P at $\boldsymbol{q}$. $P(\boldsymbol{q}) = P(x, y)$ is to be determined. Nevertheless, we shall assume that the value of $P(\boldsymbol{q}) = P(x, y)$ is known to us at this moment so we can use this value and four other values as interpolation conditions to construct a quartic curve $f_i(t)$. The five interpolation conditions are $F(\boldsymbol{v}_i)$, $\frac{\partial F(\boldsymbol{v}_i)}{\partial n_i}$, $P(\boldsymbol{q})$, $F(\boldsymbol{q}_i)$ and $\frac{\partial F(\boldsymbol{q}_i)}{\partial n_i}$ at $\boldsymbol{v}_i$, $\boldsymbol{q}$ and $\boldsymbol{q}_i$, respectively, as shown in Fig. 3. Let the distances from $\boldsymbol{v}_i$ to $\boldsymbol{q}$ and $\boldsymbol{q}_i$ be denoted by t_{i1} and t_{i2},

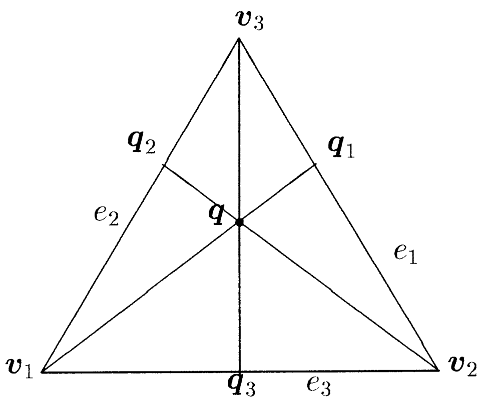

Fig. 2. The intersection points q_i.

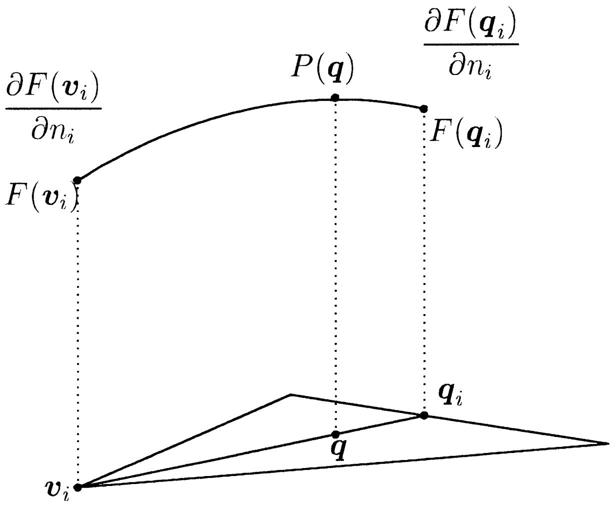

Fig. 3. A quartic interpolation curve.

respectively, then the quartic curve $f_i(t)$ that interpolates the above five interpolation conditions can be defined as follows:

$$f_i(t) = N_i(t) + \left[P(\boldsymbol{q}) - N_i(t_{i1})\right]\frac{t^2(t-t_{i2})^2}{t_{i1}^2(t_{i1}-t_{i2})^2}, \quad i = 1, 2, 3, \tag{1}$$

where t is the parameter and $N_i(t)$ are Nielson's Hermite (side-vertex) interpolation operators (Nielson, 1979),

$$N_i(t) = H_0\left(\frac{t}{t_{i2}}\right)F(\boldsymbol{v}_i) + H_1\left(\frac{t}{t_{i2}}\right)t_{i2}\frac{\partial F(\boldsymbol{v}_i)}{\partial n_i} + H_2\left(\frac{t}{t_{i2}}\right)F(\boldsymbol{q}_i) + H_3\left(\frac{t}{t_{i2}}\right)t_{i2}\frac{\partial F(\boldsymbol{q}_i)}{\partial n_i}, \tag{2}$$

with

$$\begin{aligned} &H_0(s) = (s-1)^2(2s+1), && H_1(s) = (s-1)^2 s,\\ &H_2(s) = s^2(-2s+3), && H_3(s) = s^2(s-1), \end{aligned}$$

being cubic Hermite basis functions on [0, 1].

The quartic curve $f_i(t)$, $i=1,2,3$, satisfies the following interpolation conditions:

$$\begin{aligned}
&f_i(0)=F(\boldsymbol{v}_i), \quad \frac{\mathrm{d}f_i(0)}{\mathrm{d}t}=\frac{\partial F(\boldsymbol{v}_i)}{\partial n_i};\\
&f_i(t_{i1})=P(\boldsymbol{q});\\
&f_i(t_{i2})=F(\boldsymbol{q}_i), \quad \frac{\mathrm{d}f_i(t_{i2})}{\mathrm{d}t}=\frac{\partial F(\boldsymbol{q}_i)}{\partial n_i}.
\end{aligned}$$

The unknown $P(\boldsymbol{q})=P(x,y)$ is the intersection point of the curves $f_1(t)$, $f_2(t)$ and $f_3(t)$ at $\boldsymbol{q}$. Its value is determined by requiring these curves to be tangent to the same plane at $\boldsymbol{q}$. The solution will be discussed in Section 3.2.

Note: As $\boldsymbol{q}=(x,y)$ being an arbitrary point of T, $f_i(t)$ and $N_i(t)$ are actually surfaces. When t takes on the value of t_{i1}, one gets two surfaces $P(x,y)$ and $N_i(x,y)$ from (1) and (2), respectively.

3.2. Constructing interior interpolation operator

As $t_{i1}/t_{i2}=1-L_i$, the derivative of $f_i(t)$ defined in (1) along the direction n_i at point $t=t_{i1}$ is

$$\frac{\mathrm{d}f_i(t_{i1})}{\mathrm{d}t}=P(\boldsymbol{q})A_i-B_i, \tag{3}$$

where

$$\begin{aligned}
A_i&=\frac{2(2L_i-1)}{L_i(1-L_i)}t_{i2},\\
B_i&=N_i(t_{i1})A_i-\frac{\mathrm{d}N_i(t_{i1})}{\mathrm{d}t}
\end{aligned} \tag{4}$$

with

$$\begin{aligned}
N_i(t_{i1})=N_i(x,y) &= H_0(1-L_i)F(\boldsymbol{v}_i)+H_1(1-L_i)t_{i2}\frac{\partial F(\boldsymbol{v}_i)}{\partial n_i}\\
&\quad+H_2(1-L_i)F(\boldsymbol{q}_i)+H_3(1-L_i)t_{i2}\frac{\partial F(\boldsymbol{q}_i)}{\partial n_i},\\
\frac{\mathrm{d}N_i(t_{i1})}{\mathrm{d}t}=\frac{\mathrm{d}N_i(x,y)}{\mathrm{d}t} &= H_0'(1-L_i)\frac{F(\boldsymbol{v}_i)}{t_{i2}}+H_1'(1-L_i)\frac{\partial F(\boldsymbol{v}_i)}{\partial n_i}\\
&\quad+H_2'(1-L_i)\frac{F(\boldsymbol{q}_i)}{t_{i2}}+H_3'(1-L_i)\frac{\partial F(\boldsymbol{q}_i)}{\partial n_i}.
\end{aligned}$$

The unknown $P(x,y)$ is the intersection point of these curves at $\boldsymbol{q}$. Its value is determined by requiring $f_1(t)$, $f_2(t)$ and $f_3(t)$ to have the same tangent plane at $\boldsymbol{q}$. Namely, by solving the following equation

$$\left[\left(\frac{\mathrm{d}f_1(t_{i1})}{\mathrm{d}n_1}\times\frac{\mathrm{d}f_2(t_{i1})}{\mathrm{d}n_2}\right)\cdot\frac{\mathrm{d}f_3(t_{i1})}{\mathrm{d}n_3}\right]=0 \tag{5}$$

where $(\boldsymbol{a}\times\boldsymbol{b})$ denotes the cross product of vectors $\boldsymbol{a}$ and $\boldsymbol{b}$, $[\boldsymbol{a}.\boldsymbol{b}]$ is the dot product of vectors $\boldsymbol{a}$ and $\boldsymbol{b}$. The solution of (5) is

$$P(x,y)=\frac{K_1(x,y)B_1+K_2(x,y)B_2+K_3(x,y)B_3}{K_1(x,y)A_1+K_2(x,y)A_2+K_3(x,y)A_3}, \tag{6}$$

where

$$\begin{aligned}
K_1(x,y) = {} & \frac{L_1(x_1-x_2)+L_3(x_3-x_2)}{t_{22}(L_1+L_3)}\,\frac{L_1(y_1-y_3)+L_2(y_2-y_3)}{t_{32}(L_1+L_2)} \\
& - \frac{L_1(x_1-x_3)+L_2(x_2-x_3)}{t_{32}(L_1+L_2)}\,\frac{L_1(y_1-y_2)+L_3(y_3-y_2)}{t_{22}(L_1+L_3)}, \\
K_2(x,y) = {} & \frac{L_1(x_1-x_3)+L_2(x_2-x_3)}{t_{32}(L_1+L_2)}\,\frac{L_2(y_2-y_1)+L_3(y_3-y_1)}{t_{12}(L_2+L_3)} \\
& - \frac{L_2(x_2-x_1)+L_3(x_3-x_1)}{t_{12}(L_2+L_3)}\,\frac{L_1(y_1-y_3)+L_2(y_2-y_3)}{t_{32}(L_1+L_2)}, \\
K_3(x,y) = {} & \frac{L_2(x_2-x_1)+L_3(x_3-x_1)}{t_{12}(L_2+L_3)}\,\frac{L_1(y_1-y_2)+L_3(y_3-y_2)}{t_{22}(L_1+L_3)} \\
& - \frac{L_1(x_1-x_2)+L_3(x_3-x_2)}{t_{22}(L_1+L_3)}\,\frac{L_2(y_2-y_1)+L_3(y_3-y_1)}{t_{12}(L_2+L_3)},
\end{aligned}$$

and A_i, and B_i, $i=1,2,3$, are defined in (4). Note that from (4) and (6) it is easy to see that $P(x,y)$ is indeed a function of x and y. $P(x,y)$ is called an *interior interpolation operator.*

Theorem 1. *$P(x,y)$ defined by* (6) *interpolates the given boundary curves of T, and reproduces polynomial surfaces of degree four.*

Proof. By symmetry, it is sufficient to show that $P(x,y)$ interpolates the given boundary curve on e_3 only. For e_3, we have $L_3=0$ and

$$\begin{aligned}
& N_1(x,y) = N_2(x,y), \\
& \frac{\mathrm{d}N_1(x,y)}{\mathrm{d}t} = -\frac{\mathrm{d}N_2(x,y)}{\mathrm{d}t}, \\
& K_1(x,y) = K_2(x,y), \\
& A_1 = -A_2, \\
& B_1 = -B_2.
\end{aligned}$$

Thus

$$P(x,y)|_{L_3=0} = \frac{B_3}{A_3}\bigg|_{L_3=0} = N_3(x,y)|_{L_3=0}.$$

Since $N_3(x,y)$ satisfies the given interpolation condition $F(x,y)$ on $L_3=0$, one gets $P(x,y)=F(x,y)$.

If $F(x,y)$ is a quartic polynomial, then $F(x,y)$ is a quartic curve along the n_i direction. A quartic curve can be determined by five interpolation conditions uniquely. Therefore, with the fact that $P(x,y)=F(x,y)$ in (1), $f_i(t)$ would be exactly the same as $F(x,y)$ along the n_i direction and, consequently, would be tangent to the tangent plane of the surface $F(x,y)$ at $t=t_{i1}$, $i=1,2,3$. The solution of Eq. (5) is unique, so we have $P(x,y)=F(x,y)$ for any (x,y) of T. This completes the proof of the theorem. □

It can be shown that, in general, $P(x,y)$ defined by (6) does not interpolate the given cross-boundary slopes of T. The process of constructing a C^1 triangular patch on T will be discussed in the next section.

However, it should be pointed out that if a C^0 triangular patch is all we need, then $f_i(t)$ can be defined as follows

$$f_i(t) = N_i(t) + \big[P(\boldsymbol{q}) - N_i(t_{i1})\big]\frac{t(t-t_{i2})}{t_{i1}(t_{i1}-t_{i2})},$$

where

$$N_i(t) = \left(1 - \frac{t}{t_{i2}}\right)F(\boldsymbol{v}_i) + \frac{t}{t_{i2}}F(\boldsymbol{q}_i).$$

In this case, $P(x, y)$ defined by (6) reproduces polynomial surfaces of degree two.

4. Construction of C^1 triangular patch on T

In this section we discuss the construction process of a C^1 triangular function patch using combination of four interpolation operators.

In (2), when t takes on the value of t_{i1}, one gets three *surface patches* $N_1(x, y)$, $N_2(x, y)$ and $N_3(x, y)$. The side-vertex interpolation operator $N_i(x, y)$ satisfies the given interpolation conditions on e_i. Hence, the shape of $N_i(x, y)$ in the area close to e_i is dominated by the given interpolation conditions. $P(x, y)$, on the other hand, is constructed to reproduce polynomial surfaces of degree four. It has better approximation precision than $N_i(x, y)$ on the interior of T, in terms of error in the associated Taylor series. The triangular patch $P_T(x, y)$ on T will be constructed in a way so that along and near the side e_i, $N_i(x, y)$ has a bigger influence on $P_T(x, y)$, while in the interior of T, $P(x, y)$ has a bigger influence on $P_T(x, y)$. $P_T(x, y)$ is defined as follows:

$$P_T(x, y) = w_1N_1(x, y) + w_2N_2(x, y) + w_3N_3(x, y) + w_cP(x, y), \tag{7}$$

where

$$\begin{aligned} w_1 &= L_2^2L_3^2/W_t, \\ w_2 &= L_3^2L_1^2/W_t, \\ w_3 &= L_1^2L_2^2/W_t, \\ w_c &= 27L_1L_2L_3/W_t, \\ W_t &= L_2^2L_3^2 + L_3^2L_1^2 + L_1^2L_2^2 + 27L_1L_2L_3, \end{aligned} \tag{8}$$

$N_i(x, y)$ are defined in (2) and $(L_1,\ L_2,\ L_3)$ are the barycentric coordinates of $\boldsymbol{q} = (x, y)$.

The weight functions w_1, w_2 and w_3 have properties similar to the ones defined in (Nielson, 1987), i.e., on the side e_i, $w_i = 1$, and $w_j = w_c = 0$ when $j \neq i$. The value of w_c is bigger than w_1, w_2 and w_3 for points close to the center of the T. Therefore, $P(x, y)$ has a bigger influence on the shape of $P_T(x, y)$ on the interior of T while $N_i(x, y)$ have bigger influence on the shape of $P_T(x, y)$ for areas close to the sides of T.

The factor 27 in the definition of w_c is actually a degree of freedom. Its role is to ensure that $P(x, y)$ has a bigger influence on $P_T(x, y)$ in the interior of T. The influence of w_c on the shape of $P_T(x, y)$ has been examined using the data sets shown in Section 5. The experiment results show that using numbers bigger than 24 does not improve the result any further, i.e., the shape of the constructed surface visually has no difference when the number is bigger than 24. Its value is set to 27 because at the center of T, we have $27L_1L_2L_3 = 1$. Note that, with 27, we have $w_1 = w_2 = w_3 = 1/84$ and $w_c = 81/84$ at the center of T. Hence, $P(x, y)$ indeed would have a bigger influence on the value of $P_T(x, y)$ on the interior of T.

As the shape of $P_T(x, y)$ is mainly determined by $P(x, y)$, $N_i(x, y)$, $i = 1, 2, 3$, can be regarded as transition surface patches whose roles are to make the connection of $P_T(x, y)$ with adjacent surface patches smooth.

Theorem 2. *The triangular patch $P_T(x, y)$ defined by* (7) *interpolates the given boundary curves and cross-boundary slopes on T.*

Proof. We first prove that $P_T(x, y)$ interpolates the given boundary curves at interior points of the sides of T. By symmetry, it is sufficient to show that $P_T(x, y)$ satisfies the given interpolation conditions on e_3 only.

First, note that $L_3 = 0$ on e_3. Hence, $w_1 = w_2 = w_c = 0$ and $w_3 = 1$. Consequently, $P_T(x, y)|_{L_3=0} = N_3(x, y)|_{L_3=0}$. Therefore, $P_T(x, y)$ interpolates the given boundary curve on the interior of e_3.

Next, we show that $P_T(x, y)$ interpolates the given cross-boundary slope on the interior of e_3. For a given direction vector l, let $\frac{\partial}{\partial l}$ denote the first partial derivative with respect to l.

As $L_3 = 0$, we have,

$$
\begin{aligned}
& w_c|_{L_3=0} = \left.\frac{\partial w_1}{\partial l}\right|_{L_3=0} = \left.\frac{\partial w_2}{\partial l}\right|_{L_3=0} = 0, \\
& w_3|_{L_3=0} = 1.
\end{aligned}
$$

Thus

$$
\left.\frac{\partial P_T(x, y)}{\partial l}\right|_{L_3=0} = \left.\left\{N_3(x, y)\frac{\partial w_3}{\partial l} + P(x, y)\frac{\partial w_c}{\partial l} + \frac{\partial N_3(x, y)}{\partial l}\right\}\right|_{L_3=0}.
$$

Since $w_1 + w_2 + w_3 + w_c = 1$, and $N_3(x, y)$ and $P(x, y)$ have the same value on $L_3 = 0$, one gets

$$
\begin{aligned}
\left.\left\{N_3(x, y)\frac{\partial w_3}{\partial l} + P(x, y)\frac{\partial w_c}{\partial l}\right\}\right|_{L_3=0} &= \left.N_3(x, y)\frac{\partial}{\partial l}(w_3 + w_c)\right|_{L_3=0} \\
&= \left.N_3(x, y)\frac{\partial}{\partial l}(w_1 + w_2 + w_3 + w_c)\right|_{L_3=0} = 0.
\end{aligned}
$$

Hence,

$$
\left.\frac{\partial P_T(x, y)}{\partial l}\right|_{L_3=0} = \left.\frac{\partial N_3(x, y)}{\partial l}\right|_{L_3=0}.
$$

So, $P_T(x, y)$ interpolates the given boundary curves and cross-boundary slopes on the three sides of T except the three vertices of T.

On the other hand, it is easy to see that $N_1(x, y)$, $N_2(x, y)$, $N_3(x, y)$ and $P(x, y)$ interpolate the given function values and first derivatives at the vertices of T. So, their combination $P_T(x, y)$ interpolates the given function values and first derivatives at the vertices of T as well.

Consequently, $P_T(x, y)$ interpolates the given boundary curves and cross-boundary slopes on the three sides of T. This completes the proof of the theorem. □

Remark. $N_1(x,y)$, $N_2(x,y)$, $N_3(x,y)$ and $P(x,y)$ are (at least) C^1 continuous on T and interpolates the given function value and first derivatives at the vertex (x_1,y_1) of T. So, for any $\varepsilon>0$, there is $\delta>0$, such that when $|x_1-x|<\delta$ and $|y_1-y|<\delta$, we have

$$\left|\frac{\partial^n P(x,y)}{\partial l^n}-\frac{\partial^n F(x_1,y_1)}{\partial l^n}\right|<\varepsilon,\quad n=0,1$$

and

$$\left|\frac{\partial^n N_i(x,y)}{\partial l^n}-\frac{\partial^n F(x_1,y_1)}{\partial l^n}\right|<\varepsilon,\quad n=0,1,\ i=1,2,3,$$

respectively, where $\frac{\partial}{\partial l}$ denotes the first partial derivative with respect to l. Consequently, together with the proof of Theorem 2 above, one gets that $P_T(x,y)$, the convex combination of $N_1(x,y)$, $N_2(x,y)$, $N_3(x,y)$ and $P(x,y)$, is C^1 continuous at and in the vicinity of (x_1,y_1) of T. Similarly, $P_T(x,y)$ is C^1 continuous at and in the vicinity of (x_2,y_2) and (x_3,y_3) of T. Therefore, the surface patch $P_T(x,y)$ is C^1 continuous on T. □

As $N_i(x,y)$, $i=1,2,3$, can only reproduce cubic polynomials, the polynomial interpolation precision of $P_T(x,y)$ is one degree lower than $P(x,y)$. One can make $P_T(x,y)$ have the same polynomial interpolation precision as $P(x,y)$ by defining w_i, $i=1,2,3$, and w_c as follows:

$$\begin{aligned}
w_1 &= c_1L_2^2L_3^2/W_t,\\
w_2 &= c_2L_3^2L_1^2/W_t,\\
w_3 &= c_3L_1^2L_2^2/W_t,\\
w_c &= 27(1+c_1+c_2+c_3)L_1L_2L_3/W_t,\\
W_t &= c_1L_2^2L_3^2+c_2L_3^2L_1^2+c_3L_1^2L_2^2+27(1+c_1+c_2+c_3)L_1L_2L_3,
\end{aligned}\tag{9}$$

where

$$c_i=\int_{e_i}\left\{\frac{\partial P(x,y)}{\partial\tau_i}-\frac{\partial F(x,y)}{\partial\tau_i}\right\}^2\mathrm{d}e_i$$

is an integral along the side e_i, with τ_i being the unit outward normal vector of e_i. If $F(x,y)$ is a polynomial of degree four, we have $c_i=0$, $i=1,2,3$. Consequently, $P_T(x,y)=P(x,y)$.

5. Experiment

In the design of free-form surfaces, isophotes (Poeschl, 1984), reflection lines (Klass, 1980) and highlight lines (Beier and Chen, 1994) have been proved to be effective tools in assessing the quality of a surface. In this section, the highlight line model is used to compare the new method with Nielson's approach (Theorem 3.1 of (Nielson, 1979)) that interpolate both the boundary curves and cross-boundary slopes. Nielson's approach reproduces cubic polynomial surfaces. The weight functions for the new method are defined by (8). Six bi-variate functions proposed by Franke (1979) are used in the comparison process. They are

$$
\begin{aligned}
F_1(x,y) = {} & 3.9\exp\bigl[-0.25(9x-2)^2-0.25(9y-2)^2\bigr] \\
& + 3.9\exp[-(9x+1)^2/49-(9y+1)/10\bigr] \\
& + 2.6\exp\bigl[-0.25(9x-7)^2-0.25(9y-3)^2\bigr] \\
& - 1.04\exp\bigl[-(9x-4)^2-(9y-7)^2\bigr], \\
F_2(x,y) = {} & 5.2\exp\bigl[18y-18x]/\bigl(9\exp[18y-18x]+9\bigr), \\
F_3(x,y) = {} & 5.2\bigl[1.25+\cos(5.4y)\bigr]/\bigl[64-6(3x-1)^2\bigr], \\
F_4(x,y) = {} & 5.2\exp\bigl[-81\bigl((x-0.5)^2+(y-0.5)^2\bigr)/16\bigr]/3, \\
F_5(x,y) = {} & 5.2\exp\bigl[-81\bigl((x-0.5)^2-(y-0.5)^2\bigr)/4\bigr]/3, \\
F_6(x,y) = {} & 5.2\mathrm{sqrt}\bigl[64-81\bigl((x-0.5)^2+(y-0.5)^2\bigr)\bigr]/9-2.6.
\end{aligned}
$$

The set of data points (including 33 points) presented in (Franke, 1979) is used to produce triangles for comparison. The triangulation of the data set is performed using the max-min criterion proposed by Lawson (1977) (see Fig. 4).

The interpolation conditions for the test cases are boundary curves and cross-boundary slopes on the sides of the triangles, taken from $F_1(x,y)$ to $F_6(x,y)$ above. The comparison results are shown in Figs. 5–9. For each case in Figs. 5–9, the surface is shown in two models: wireframe model (left) and highlight line model (right) (with 11 linear light sources for Figs. 5 and 11, and 20 linear light sources for the remaining cases). Actually the ones shown on the right side of Fig. 5 are orthographic projections of the highlight line models on xy plane. The wireframe models of the surfaces generated by our method and Nielson's method have no obvious difference visually, but the highlight line models have obvious differences.

The results for $F_6(x,y)$ are not shown because the surfaces by both methods are satisfactory and they have no visual difference.

The surfaces produced by both methods for $F_1(x,y)$ and $F_2(x,y)$ are not satisfactory, this is because the given interpolation conditions are not fine enough for regions with large curvature. We further test the two methods by increasing the interpolation conditions, i.e., adding new data points into the 33-point data set. We first add 17 data points into Fig. 4 to form a set of 50 data points. This is done by putting 8 points on the boundary edges and 9 points inside the square. The 9 points put inside the square are

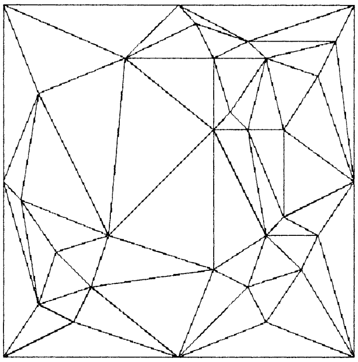

Fig. 4. Triangulation of 33 points.

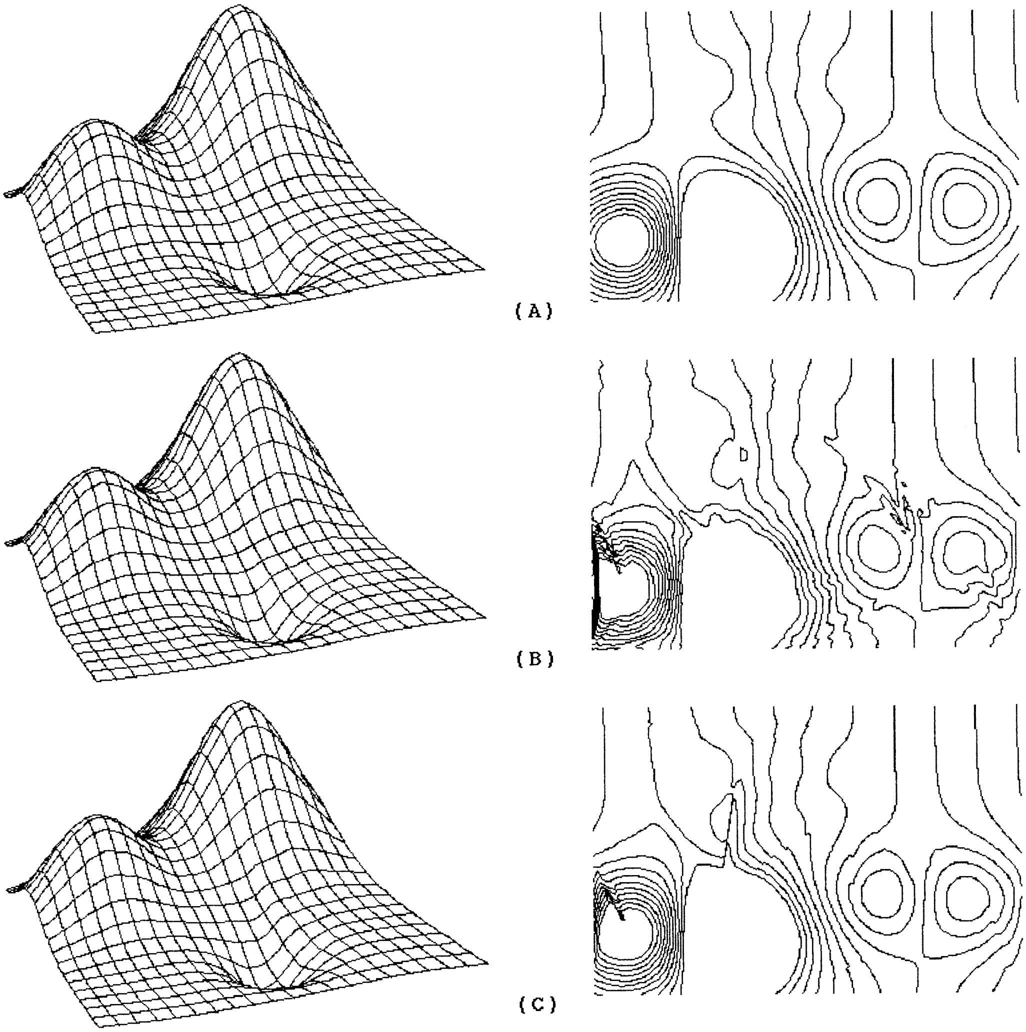

Fig. 5. (A) $F_1(x, y)$, (B) by Nielson's method, (C) by new method.

planted one at a time in the following way: triangulate the current data set, identify the triangle with the largest area, put a point at the center of the triangle, and then repeat the same process until all the 9 points are planted. The triangulation of the new data set (50 data points) is shown in Fig. 10. For $F_1(x, y)$ and $F_2(x, y)$, the surfaces produced by the two methods over the new triangles are shown in Figs. 11–12. Note that the highlight line model of the surface generated by our method for $F_1(x, y)$ is visually the same as the highlight line model of $F_1(x, y)$. The surfaces produced by both methods for $F_2(x, y)$ are not satisfactory. We then add 67 data points into Fig. 4 to form a set of 100 data points using a similar approach. The surfaces generated by both methods for $F_2(x, y)$ are shown in Fig. 13. The highlight line model of the surface generated by our method for $F_2(x, y)$ now is visually the same as the highlight line model of $F_2(x, y)$.

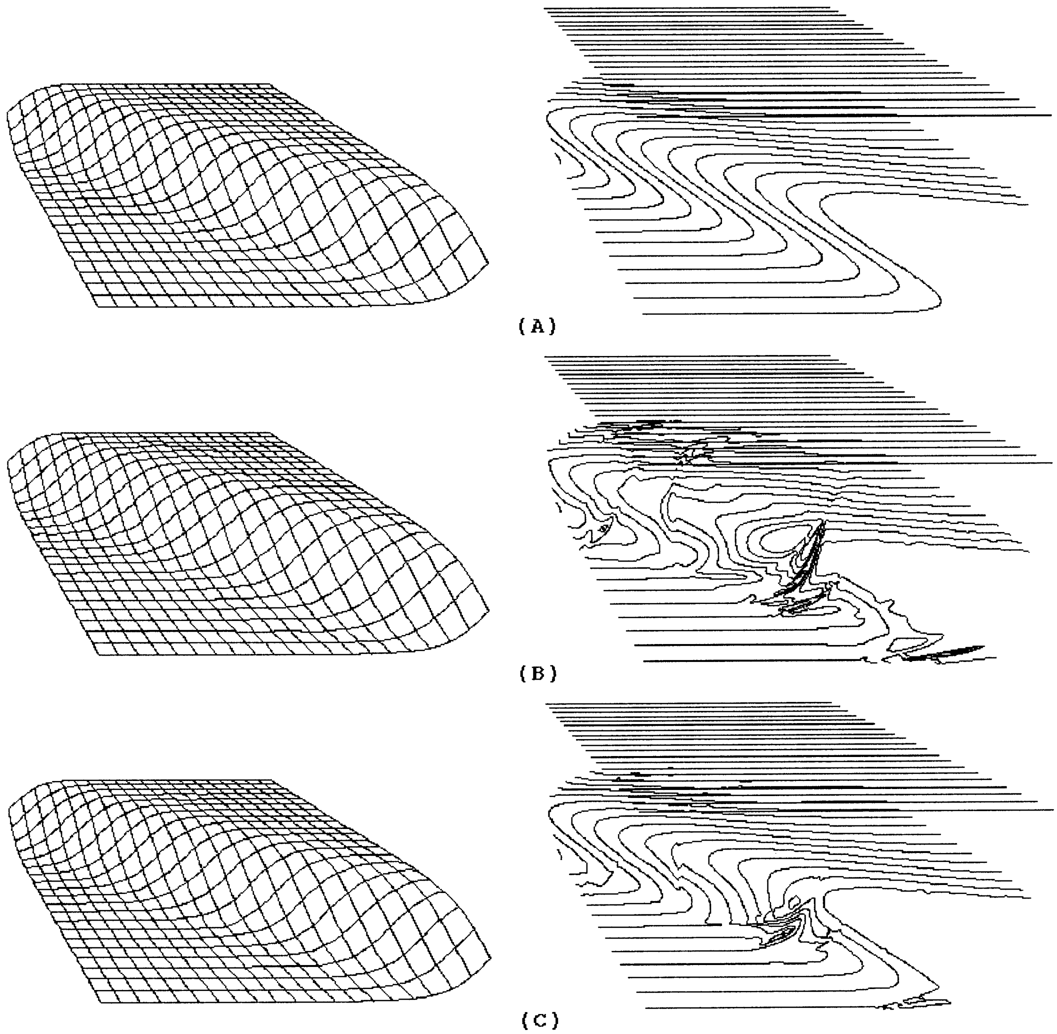

Fig. 6. (A) $F_2(x, y)$, (B) by Nielson's method, (C) by new method.

Table 1
Computation times

Time	$F_1(x, y)$	$F_2(x, y)$	$F_3(x, y)$	$F_4(x, y)$	$F_5(x, y)$
Original function (A)	44T	36T	38T	36T	38T
Nielson's method (B)	80T	64T	62T	60T	62T
New method (C)	84T	64T	62T	62T	62T

The computation times for producing the (left) wireframe drawings in Figs. 5–9 are given in Table 1. Table 1 shows that the computation costs of the new method and Nielson's method are nearly the same. In fact, for both methods, the main cost is the computation of the interpolation conditions.

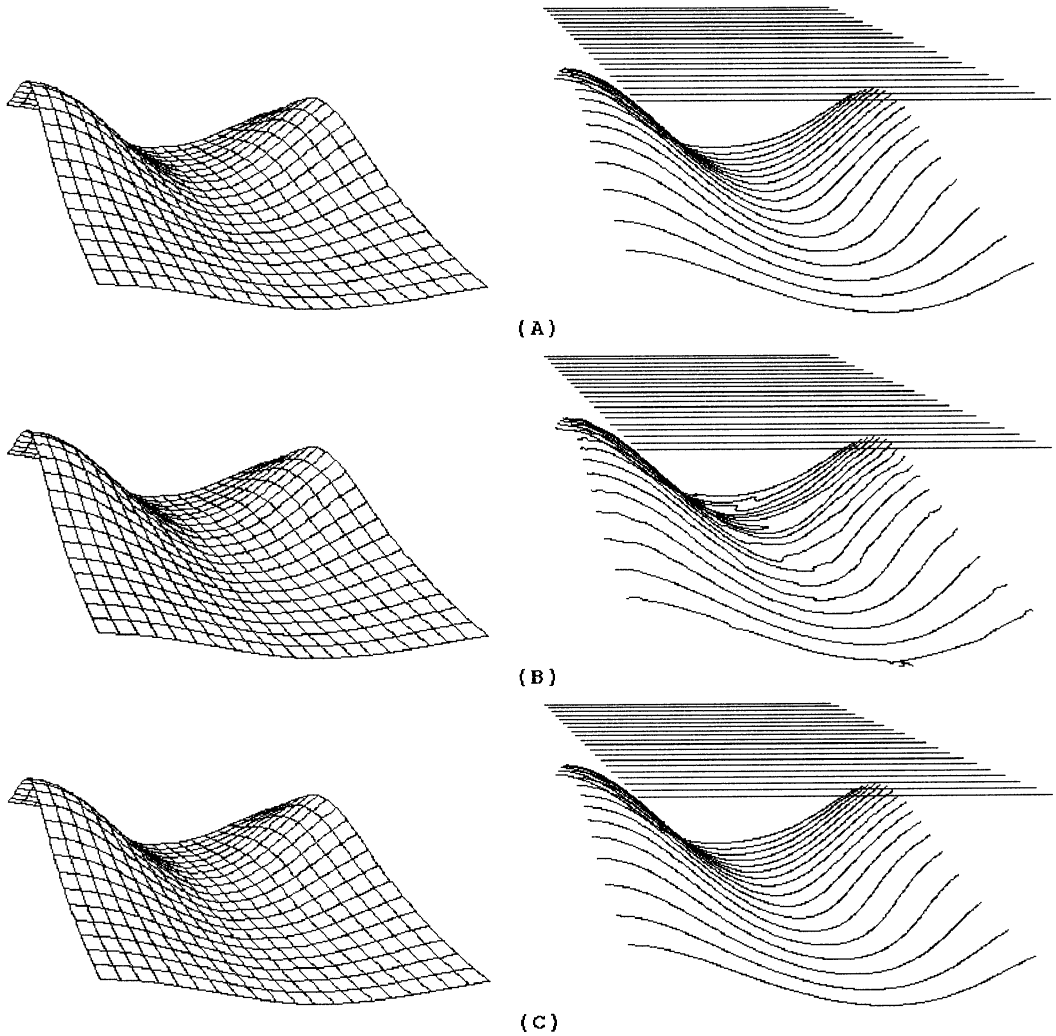

Fig. 7. (A) $F_3(x, y)$, (B) by Nielson's method, (C) by new method.

Table 2
Maximum errors generated by the three methods using 33 data points

Error	$F_1(x, y)$	$F_2(x, y)$	$F_3(x, y)$	$F_4(x, y)$	$F_5(x, y)$	$F_5(x, y)$
Nielson method	2.162e−2	1.346e−2	6.101e−3	1.882e−2	2.705e−3	8.498e−4
New method	2.876e−2	8.342e−3	2.316e−3	4.704e−3	2.841e−4	2.253e−4
$P(x, y)$	2.920e−2	8.712e−3	2.200e−3	4.899e−3	3.500e−4	2.584e−4

The interior interpolant $P(x, y)$ defined by (6) is also compared with the new method and Nielson's method. The result is that the plots of the interior interpolant $P(x, y)$ are visually the same as the ones produced by the new method. As an example, the plots produced by $P(x, y)$ for $F_3(x, y)$ and $F_5(x, y)$ are shown in Figs. 14–15. Based on the triangulations shown in Figs. 4 and 10, the errors of the three

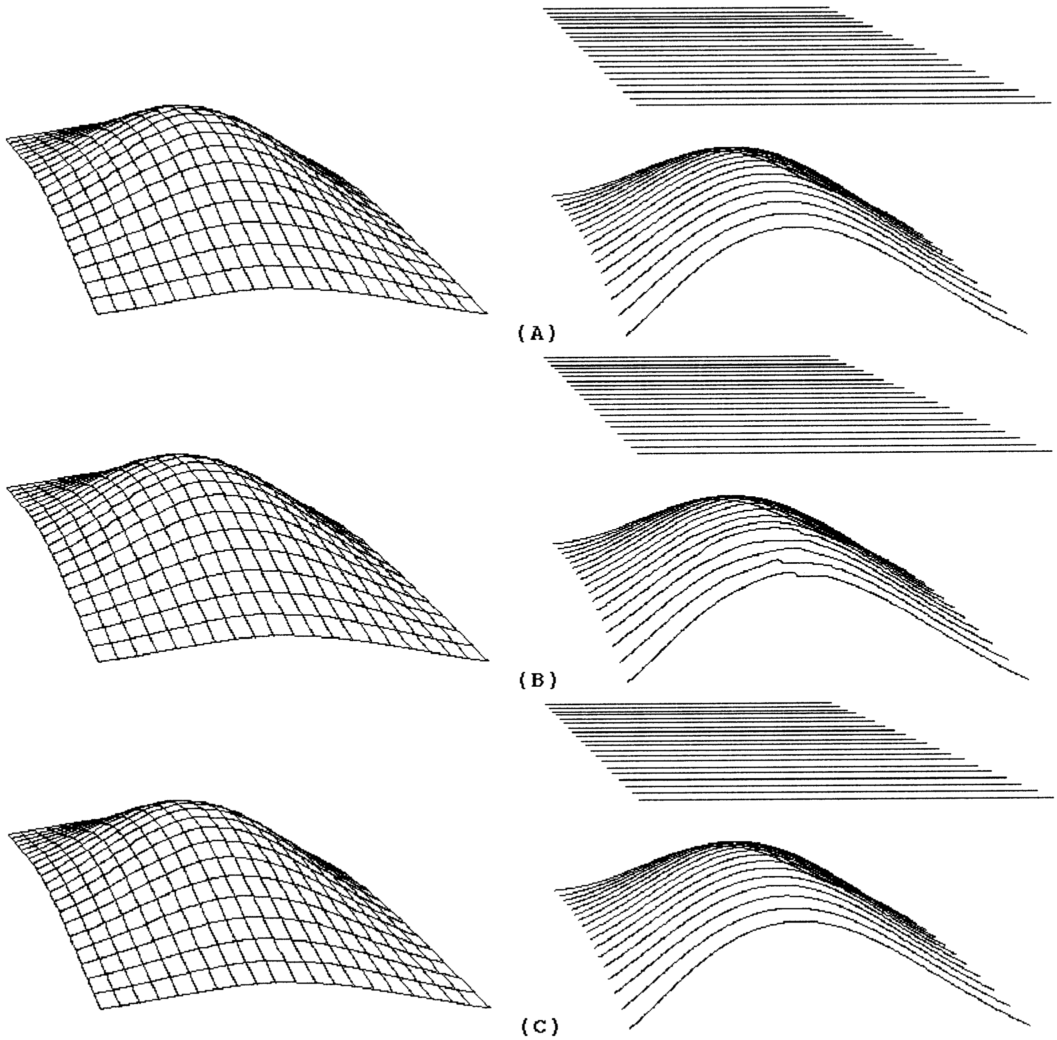

Fig. 8. (A) $F_4(x, y)$, (B) by Nielson's method, (C) by new method.

Table 3
Maximum errors generated by the three methods using 50 data points

Error	$F_1(x, y)$	$F_2(x, y)$	$F_3(x, y)$	$F_4(x, y)$	$F_5(x, y)$	$F_5(x, y)$
Nielson method	4.528e−3	5.601e−3	1.089e−3	3.001e−3	2.170e−4	1.554e−4
New method	9.394e−4	2.660e−3	2.078e−4	3.269e−4	2.315e−5	2.621e−5
$P(x, y)$	8.957e−4	2.875e−3	1.818e−4	3.334e−4	2.446e−5	3.180e−5

methods for interpolating $F_1(x, y)$–$F_6(x, y)$ are given in Tables 2 and 3, respectively. Tables 2 and 3 show that $P_T(x, y)$ (7) has generally better precision than $P(x, y)$ (6).

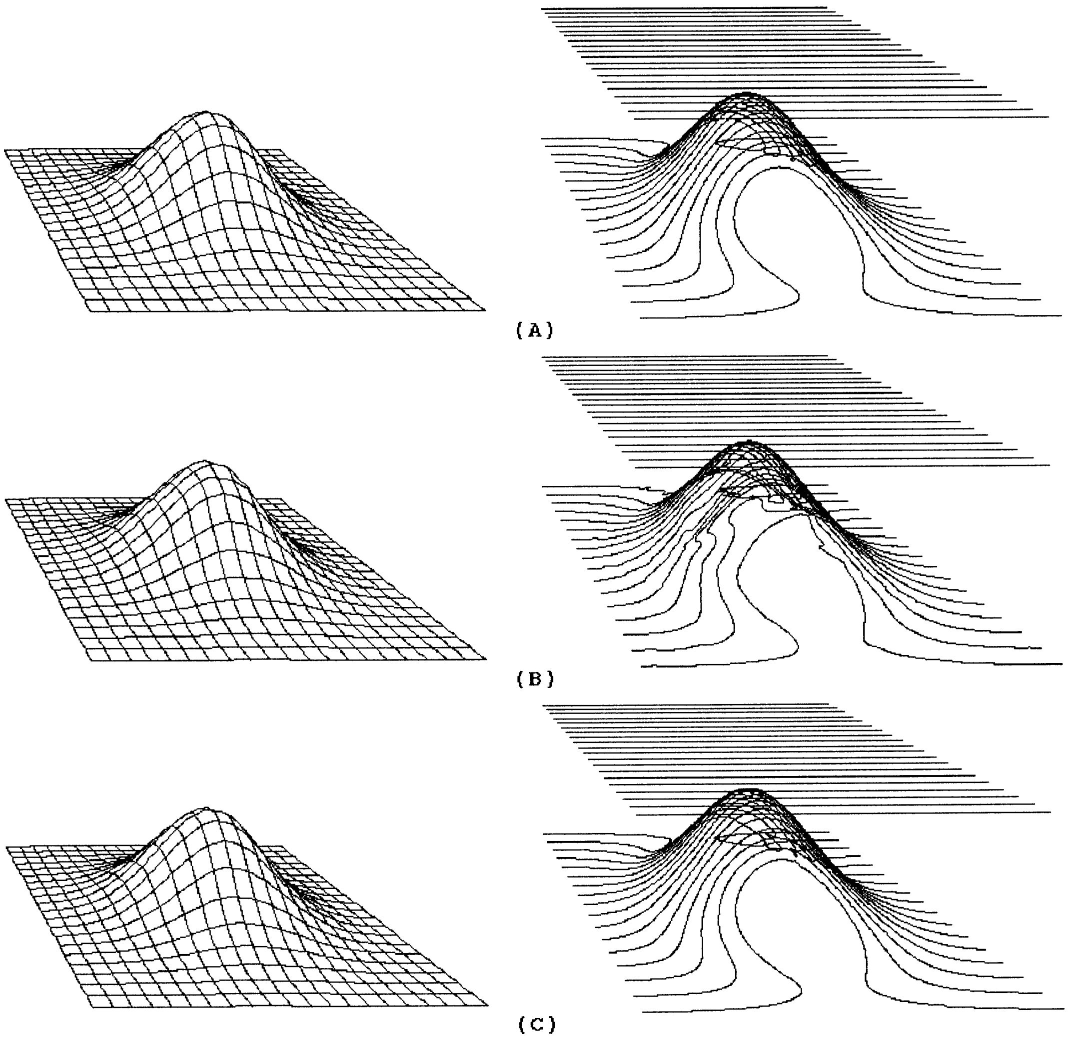

Fig. 9. (A) $F_5(x, y)$, (B) by Nielson's method, (C) by new method.

Using the above examples we have also compared the two weight functions defined by (8) and (9). The test results show that they produce similar results. The reason is because either case would make $P(x, y)$ the dominant factor in determining the value and, consequently, the shape of $P_T(x, y)$.

6. Conclusions

A new method to construct C^1 triangular patches by combining four interpolation operators is presented. The interpolation operators include an interior interpolation operator and three Nielson type side-vertex interpolation operators. The interior interpolation operator has a better approximation precision on the interior of the triangular domain than the side-vertex interpolation operators. Since the

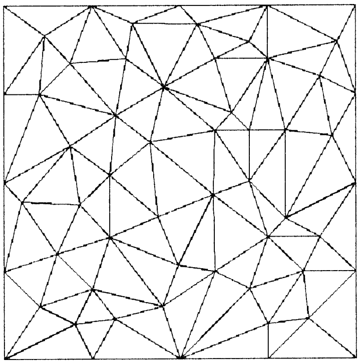

Fig. 10. Triangulation of 50 points.

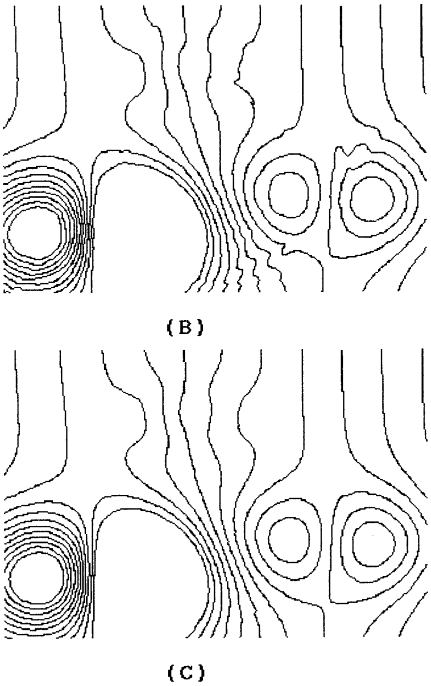

Fig. 11. Interpolants to $F_1(x, y)$, (B) by Nielson's method, (C) by new method.

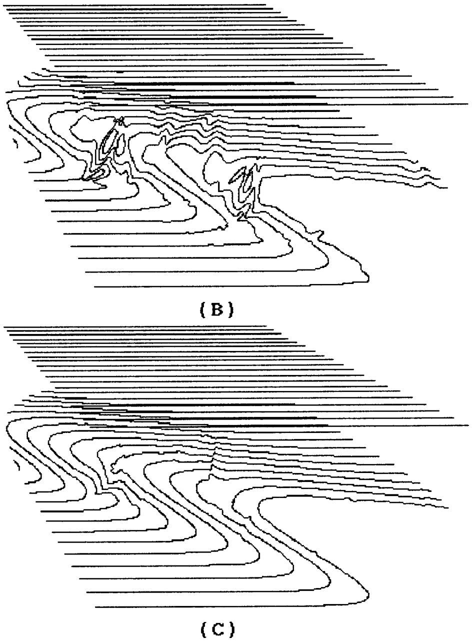

Fig. 12. Interpolants to $F_2(x, y)$, (B) by Nielson's method, (C) by new method.

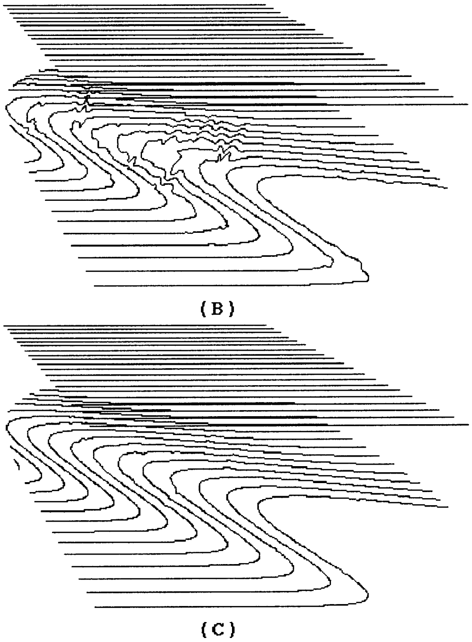

Fig. 13. Interpolants to $F_2(x, y)$, (B) by Nielson's method, (C) by new method.

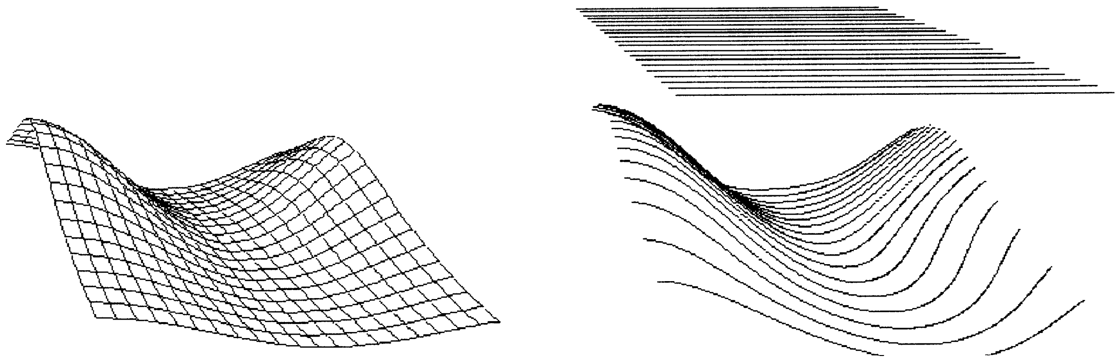

Fig. 14. Interior interpolation surface of $F_3(x, y)$.

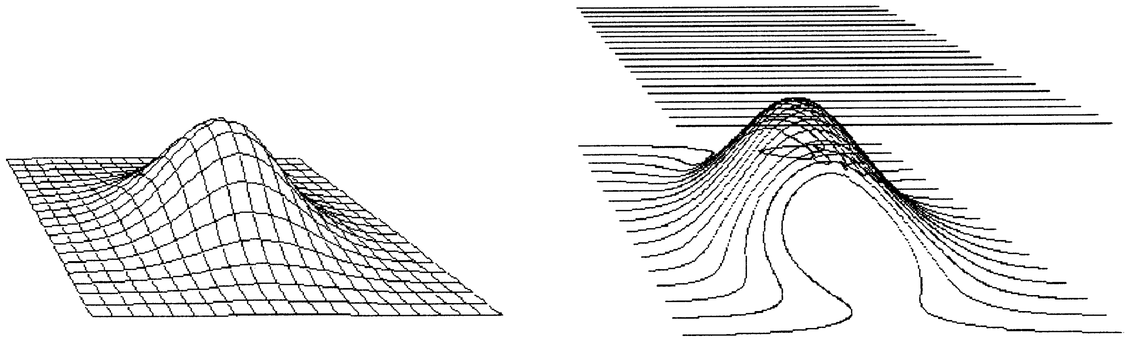

Fig. 15. Interior interpolation surface of $F_5(x, y)$.

interior interpolation operator plays a dominant role in the combination process, the resulting triangular patch has better approximation precision than the one produced by Nielson's approach. Our test results also show that the surfaces produced by the new method are visually smoother than the ones produced by Nielson's approach.

The new method can be easily extended to construct C^2 triangular patches as well—simply replace Nielson's side-vertex interpolation operators with Hagen's operators (Hagen, 1986). The constructed triangular patch in this case reproduces polynomial surfaces of degree six.

It seems possible to generalize this method to cover parametric triangular patches. The main concern is how to apply the scheme for the parametric case while holding the interpolation precision of the scheme unchanged. This will be a future research work in this direction.

Acknowledgements

The financial support of Ford Motor Company through a URP grant and Honda Motor Company through two HIG grants, and the consulting support of Drs. Paul Stewart and Yifan Chen of the Ford Research Lab and Dr. Shane Chang of the Honda R&D North America are deeply appreciated.

We also thank the anonymous reviewers for many helpful comments on a previous version of the paper. These comments help bring the paper to its current form.

References

Barnhill, R.E., Birkhoff, G., Gordon, W.J., 1973. Smooth interpolation in triangles. J. Approx. Theory 8, 114–128.

Beier, K.-P., Chen, Y., 1994. The highlight-line algorithm for real-time surface-quality assessment. Computer-Aided Design 26, 268–278.

Charrot, P., Gregory, J.A., 1984. A pentagonal surface patch for computer aided geometric design. Computer Aided Geometric Design 1, 87–94.

Foley, T.A., Opitz, K., 1992. Hybrid cubic Bézier triangle patches. In: Lyche, T., Schumaker, L. (Eds.), Mathematical Methods for Computer Aided Geometric Design II. Academic Press, pp. 275–286.

Franke, R., 1979. A critical comparison of some methods for interpolation of scattered data. Naval Postgraduate school, Technical Report NPS-53-79-003.

Gregory, J.A., 1974. Smooth interpolation without twist constraints. In: Barnhill, R.E., Riesenfeld, R.F. (Eds.), Computer Aided Geometric Design. Academic Press, New York, pp. 71–88.

Gregory, J.A., 1983. C^1 rectangular and non-rectangular surface patches. In: Barnhill, R.E., Boehm, W. (Eds.), Surfaces in Computer Aided Geometric Design. North-Holland, Amsterdam.

Hagen, H., 1986. Geometric surface patches without twist constraints. Computer Aided Geometric Design 3, 179–184.

Hagen, H., 1989. Curvature continuous triangular interpolants. In: Lyche, T., Schumaker, L. (Eds.), Methods in CAGD. Academic Press, Oslo, pp. 373–384.

Klass, R., 1980. Correction of local surface irregularities using reflection lines. Computer-Aided Design 12, 73–76.

Kuriyama, S., 1994. Surface modeling with an irregular network of curves via sweeping and blending. Computer-Aided Design 26 (8), 597–606.

Lawson, C.L., 1977. Software for C^1 surface interpolation. In: Rice, J.R. (Ed.), Mathematical Software III. Academic Press, New York, pp. 161–194.

Nielson, G.M., 1979. The side vertex method for interpolation in triangles. J. Approx. Theory 25, 318–336.

Nielson, G.M., 1987. A transfinite, visually continuous, triangular interpolant. In: Farin, G. (Ed.), Geometric Modeling, Applications and New Trends. SIAM, Philadelphia, pp. 235–246.

Poeschl, T., 1984. Detecting surface irregularities using isophotes. Computer Aided Geometric Design 1, 163–168.

Varady, T., 1991. Overlap patches: a new scheme for interpolating curve networks with n-sided regions. Computer Aided Geometric Design 8, 7–27.

Zhang, C., Agui, T., Nagahashi, H., Nagao, T., 1993. A new method for smooth interpolation without twist constraints. IEICE Trans. Inf. Syst. E76-D, 243–250.